

# Stability and Controls Analysis and Flight Test Results of a 24-Foot Telescoping Nose Boom on an F-15B Airplane

Cheng M. Moua<sup>\*</sup>, Timothy H. Cox<sup>†</sup>, and Shaun C. McWherter<sup>‡</sup>  
*NASA Dryden Flight Research Center, Edwards, CA 93523*

The Quiet Spike™ F-15B flight research program investigated supersonic shock reduction using a 24-ft telescoping nose boom on an F-15B airplane. The program goal was to collect flight data for model validation up to 1.8 Mach. In the area of stability and controls, the primary concerns were to assess the potential destabilizing effect of the oversized nose boom on the stability, controllability, and handling qualities of the airplane and to ensure adequate stability margins across the entire research flight envelope. This paper reports on the stability and control analytical methods, flight envelope clearance approach, and flight test results of the F-15B telescoping nose boom configuration. Also discussed are brief pilot commentary on typical piloting tasks and refueling tasks.

## Nomenclature

CAP	= control anticipation parameter, $g^{-1} s^{-2}$
CAS	= control augmentation system
CFD	= computational fluid dynamics
$C_{m_q}$	= pitching moment caused by pitch rate variation, per rad/s
$C_{m_\alpha}$	= pitching moment caused by angle-of-attack variation, per deg
$C_{n_r}$	= yawing moment caused by yaw rate variation, per rad/s
$C_{n_\beta}$	= yawing moment caused by sideslip variation, per deg
DFRC	= Dryden Flight Research Center
Dif aileron	= differential aileron deflection, deg
Dif stab	= differential stabilator deflection, deg
FS	= fuselage station, in
$g$	= acceleration caused by gravity, $ft/s^2$
$\dot{H}$	= rate of decent, ft/s
$N_y$	= lateral acceleration, $ft/s^2$
$N_z$	= normal acceleration, $ft/s^2$
PID	= parameter identification
Pitch stick	= pitch stick deflection, in
$q$	= pitch rate, deg/s
QS	= Quiet Spike™
$r$	= yaw rate, deg/s
rad/s	= radians per second
spike	= Quiet Spike™
sym rudder	= symmetric rudder position, deg
sym stab	= symmetric stabilator position, deg
$\alpha$	= angle of attack, deg
$\beta$	= angle of sideslip, deg

<sup>\*</sup> Aerospace Engineer, Controls and Dynamics Branch, P.O. Box 273/MS 4840D, AIAA member.

<sup>†</sup> Aerospace Engineer, Controls and Dynamics Branch, P.O. Box 273/MS 4840D, Non-member.

<sup>‡</sup> Aerospace Engineer, Controls and Dynamics Branch, P.O. Box 273/MS 4840D, AIAA member.

$\beta \cdot \bar{q}$	= lateral load design parameter, deg lb/in <sup>2</sup>
$\Delta C_{D\alpha}$	= change in drag coefficient caused by alpha, per deg
$\Delta C_{D\beta}$	= change in drag coefficient caused by beta, per deg
$\Delta C_{L\alpha}$	= change in lift coefficient caused by alpha, per deg
$\Delta C_{m\alpha}$	= change in pitch moment caused by alpha, per deg
$\Delta C_{n\alpha}$	= change in roll moment caused by beta, per deg
$\Delta C_{y\beta}$	= change in side force caused by beta, per deg
$\phi$	= bank angle, deg
$\omega_{dr}$	= Dutch roll period
$\zeta_{dr}$	= Dutch roll damping ratio
$\zeta_{sp}$	= short period damping ratio

## I. Introduction

THE Federal Aviation Administration restricts supersonic flight, except in special military flight corridors to prevent aircraft from causing sonic booms over populated areas. This represents a significant obstacle for aircraft manufacturers to produce supersonic civilian transport aircraft. Finding a way to suppress or “soften” the sonic boom of a supersonic aircraft could open the way to the production of a new generation of supersonic civilian aircraft.

The Quiet Spike™ is a technology concept developed by Gulfstream Inc. (Savannah, Georgia) as a potential method for softening the sonic boom in smaller supersonic aircraft by partitioning the transonic shock wave into a series of smaller shock waves along a segmented boom extending from the front of an aircraft. Gulfstream Inc. approached the NASA Dryden Flight Research Center (DFRC) (Edwards, California) as a research partner to conduct flight tests of a subscale version of the Quiet Spike on an existing airplane. For the remainder of this paper, the Quiet Spike will be referred to simply as “spike.” Gulfstream provided the flight-worthy spike hardware. The DFRC was responsible for installation of the spike on the F-15B (McDonnell Douglas Aerospace, now Boeing, St. Louis, Missouri) airplane and for conducting ground test, flight test, and for range safety.

The primary objectives of the flight research program were to determine the spike’s feasibility for structural design methodologies, validate the mechanical systems, and characterize the spike’s near-field shock waves. In the area of stability and controls, the primary objectives were to assess the effect of the spike on the stability, controllability, and handling qualities of the airplane and to ensure adequate stability margins across the entire spike flight envelope. This paper reports on the stability and control methods used for flight envelope clearance, flight test results of the F-15B spike configuration, and will focus on the spike-extended configuration.

## II. Test Aircraft

The NASA DFRC F-15B airplane (Fig. 1) serves as a research test bed for various in-flight experiments. The DFRC-installed instrumentation and telemetry systems provide onboard data recording and real-time control room monitoring capability. A detailed description of the F-15B airplane can be found in NASA TM-4782.<sup>1</sup> Besides the spike, the only other modifications external to the mold line of the production F-15B airplane were the addition of a small sideslip vane to the underside just aft of the nose cone and a fiberglass fairing over the gun port.<sup>2</sup>

The flight control system is a standard F-15B integrated mechanical and control augmentation system (CAS). The CAS is a single-string system in parallel with the mechanical control system. Feedback signals for the CAS include fixed body rotation rates, accelerations, and angle of attack. Static and total pressures are utilized in the mechanical control system to modulate pitch stick path gain to improve stick response characteristics throughout the envelope. With the gear up, the CAS provides normal acceleration command in the pitch axis and roll rate in the lateral axis. With the gear down, the system provides pitch rate command. The yaw CAS provides Dutch roll damping and turn coordination through blended aircraft lateral acceleration and cancelled yaw rate from the lateral accelerometer and yaw rate gyro respectively. The CAS can be disengaged, in which case the mechanical system is

still active. All feedback is cancelled except for normal acceleration feedback in the mechanical system for the purpose of automatic trimming.

The spike consists of a 6-ft long nosecone fairing, an extendable boom (14.15 ft retracted, 24.31 ft extended), and interface attachment hardware. It attaches to the F-15B forward fuselage at the radar support bulkhead and weighs approximately 450 pounds. An electrically powered cable/pulley mechanism extends and retracts the boom. The photograph of the test airplane is shown in Fig. 1 with the spike in the fully extended position. Additional details of the spike with dimensional data are shown in Fig. 2.

### III. Simulation Description

The NASA DFRC simulation facility includes a dedicated fixed-base real-time pilot-in-the-loop F-15 simulator with standard stick and rudder pedal inceptors for pilot controls, heads up display, cockpit pilot flight instruments, and external real-time visual imagery. Oblate Earth nonlinear six-degree-of-freedom equations of motion are utilized. Four research flights were conducted, before flying the spike on the aircraft, to gather data to update the DFRC F-15B baseline simulation and to calibrate air data parameters on the aircraft. For a more detailed description of the air data calibration tests and results see Ref. 2. As a result of baseline flight parameter identification, an updated aerodynamic model was incorporated into the baseline F-15B simulation. Uncertainty in the base aircraft aerodynamic model was estimated from deviations observed in the parameter identification results. These uncertainties were incorporated in the simulation.

Three independently developed aerodynamic models of the spike were implemented into the DFRC F-15B simulation for stability and control analysis. One model was developed by Gulfstream Inc. using an Euler computational fluid dynamics (CFD) method that also incorporated some empirical corrections. A second model of the spike alone was developed at Dryden using an aerodynamic vortex lattice modeling method for a subsonic model and flat plate theory and empirical cone-cylinder drag data for a supersonic model. A third model was developed by Desktop Aeronautics Inc. (Palo Alto, California) with an Euler CFD method that included a full airplane model and a full airplane-with-spike model. The spike model was then extracted as a set of differences between the two models. All three models were incorporated as additive delta values to the baseline F-15B aerodynamic model in the simulation. These deltas were  $\Delta C_{L\alpha}$ ,  $\Delta C_{D\alpha}$ ,  $\Delta C_{D\beta}$ ,  $\Delta C_{m\alpha}$ ,  $\Delta C_{n\alpha}$ , and  $\Delta C_{y\beta}$ . Spike effects on the damping derivatives were not modeled. For a more detailed description of the aerodynamic models and the simulation implementation see Ref. 2.

### IV. Research Approach

#### A. Preflight Simulation Analysis

Extensive simulation stability analysis was conducted over a wide range of uncertainties in the aerodynamic derivatives before starting flight tests with the spike. The primary focus of preflight analysis was on the pitch and yaw axis dynamics. It was assumed that the roll axis dynamics were not significantly affected by the presence of the spike. The objective of the analysis was to evaluate the robustness of F-15B spike stability and flying qualities to the aerodynamic uncertainties throughout the spike flight envelope. Total aircraft aerodynamic uncertainty was used for the analysis, incorporating both the basic aircraft aerodynamic uncertainty and the spike aerodynamic uncertainty.

Table 1 defines a series of 12 aerodynamic stress test cases that were run in batch simulation over several different aircraft configurations and flight conditions with a set of predetermined stick and rudder pedal inputs. In each of the stress test cases, the aerodynamic uncertainties were varied in the worst-case directions in various combinations for both the spike and the baseline F-15 aerodynamic models, which effectively increased or decreased the stability and control effectiveness in the lateral/directional and longitudinal axes. These stress test cases were evaluated with CAS-on and CAS-off, for light, medium, and heavy fuel weights, with all three spike aerodynamic models, with the spike extended and, to a limited degree, with the spike retracted. In all test cases, perturbation dynamics were evaluated in each axis by reasonably sized pitch and yaw doublets.<sup>3</sup>

Metrics were defined to evaluate the simulation data for linear and nonlinear piloted simulation analysis. Linear analysis metrics were defined for nominal aerodynamic and stress cases covering stability margins, handling qualities, sideslip limits based on loads, g-limits, and stabilator trim requirements. For the CAS-on configuration, stability margin requirements for the nominal case were defined as 45° phase margin and 6 dB gain margin and for the aerodynamic stress cases as 30° phase margin and 4 dB gain margin. The CAS-off stability requirement was that the closed loop roots be stable.

**Table 1. Aerodynamic stress cases.**

Aerodynamic Stress Case	Directional Stability	Directional Control Effectiveness	Longitudinal Stability	Longitudinal Control Effectiveness	Normal Acceleration Gain
1	Decreased	Decreased	Decreased	Decreased	Same
2	Decreased	Increased	Decreased	Decreased	Same
3	Increased	Decreased	Decreased	Decreased	Same
4	Increased	Increased	Decreased	Decreased	Same
5	Decreased	Decreased	Increased	Increased	Same
6	Decreased	Increased	Increased	Increased	Same
7	Increased	Decreased	Increased	Increased	Same
8	Increased	Increased	Increased	Increased	Same
9	Decreased	Decreased	Decreased	Increased	Same
10	Decreased	Decreased	Increased	Decreased	Same
11	Decreased	Decreased	Decreased	Decreased	Increased
12	Decreased	Decreased	Increased	Increased	Decreased

Handling qualities metrics were defined to require level 1 handling qualities (or at the same level as the baseline F-15B airplane) for the nominal, CAS-on case. For stress cases with the CAS on, the handling qualities metrics were defined to provide level 2 handling qualities. For the CAS-off cases, the handling qualities were required to be controllable. In the pitch axis, control anticipation parameter (CAP) and short period damping were used as metrics. In the directional axis, Dutch roll frequency and damping were used. Table 2 defines level 1, 2, and 3 criteria used in the metric evaluations. For a general description of handling qualities metrics, see Ref. 4.

**Table 2. Handling qualities metrics.**

Level	Pitch	Yaw
1	$0.16 < CAP < 3.6$ and $0.35 < \zeta_{sp} < 1.3$	$\omega_{dr} > 1.0$ $\zeta_{dr} > 0.08$ or $\omega_{dr} \times \zeta_{dr} > 0.15$
2	$0.05 < CAP < 0.16$ or $3.6 < CAP < 10$ or $0.25 < \zeta_{sp} < 0.35$ or $1.3 < \zeta_{sp} < 2.0$	$\omega_{dr} > 0.4$ $\zeta_{dr} > 0.02$ or $\omega_{dr} \times \zeta_{dr} > 0.05$
3	$CAP < 0.05$ , $CAP > 10$ and $\zeta_{sp} < 0.15$	$\omega_{dr} > 0.4$ $\zeta_{dr} > 0$

The values listed in Table 3 were established as maneuvering limits and were used in evaluation of the nominal and stress cases. The  $\beta \cdot \bar{q}$  term is an established structural side load limit for the spike expressed in terms of sideslip angle,  $\beta$ , multiplied by dynamic pressure.

**Table 3. Simulation maneuvering limits.**

<b>Up and Away</b>	<b>Power Approach</b>
$\beta \cdot \bar{q} < 3000 \text{ lb deg/in}^2$	$\beta \cdot \bar{q} < 3000 \text{ lb deg/in}^2$
$0 < Nz < 3.0g$	$0 < Nz < 3.0g$
	$\dot{H} < 5 \text{ ft/s}$
$-5 < \alpha < 12 \text{ deg}$	$-5 < \alpha < 15 \text{ deg}$
$-60 < \phi < 60 \text{ deg}$	$-45 < \phi < 45 \text{ deg}$

After all metric violations were identified from the batch simulation, the worst cases were checked in the piloted simulation using typical flying tasks. If the metrics were maintained in the pilot-simulation check, then the check case was deemed acceptable. Through analysis of the robust test cases, the vehicle was found to have insufficient stability margin at the 1.6 and 1.8 Mach cases. Further review concluded that reducing the uncertainty estimation by 25 percent in those cases would provide an adequate stability margin. This necessitated validation of the aerodynamic parameters and associated uncertainty during envelope expansion.

For pilot-in-the-loop simulation evaluation the pilot comment criteria in Table 4 were used.

**Table 4. Pilot comment criteria.**

	<b>Nominal Case Pilot Comments</b>	<b>Stress Cases Pilot Comments</b>
CAS on	Satisfactory without improvement, or no worse than baseline F-15B	Objectionable, but control not in question
CAS off	Controllable	Controllable

### B. Flight Test Implications of Simulation Analysis

The F-15B simulation was a key tool to ensure adequate stability margin and handling qualities and was continually validated against flight data during the flight envelope clearance portion of the flight program. Reasonable matches between the simulation and flight data were required to continue flight envelope expansion. The stress analysis identified regions of aerodynamic variations on key derivatives that resulted in acceptable stability margin, handling qualities, and flight dynamics that were insensitive to CAS state. To accelerate the envelope expansion flight-testing, each of the key nominal F-15B aerodynamic derivatives was plotted against Mach number with aerodynamic variations that were evaluated in the extended-spike stress analysis. Only extended-spike analysis variations were evaluated because retracted analysis indicated a spike effect nearly the same or less than the more conservative extended results. Postflight parameter estimation of the aerodynamic derivatives obtained from flight test data were compared to aerodynamic variations. This allowed a quick evaluation on the clearance status of those conditions and provided justification to proceed to subsequent expansion points. The determination was made based on whether the flight estimated derivatives fell within the predetermined uncertainty boundaries. If the trends observed as a function of Mach number projected that subsequent Mach number expansion points fell within the regions, then the F-15B spike would be cleared to collect expansion test data at those points. If the projected trends indicated that an aerodynamic derivative fell outside the boundary, then further analysis would be warranted before it could be cleared to collect expansion test data. For a more detailed description of the simulation analysis and implications for the flight test procedure, see Ref. 3.

### C. Flight Test Approach

Flight envelope clearance was performed using a build-up approach with the spike in the extended configuration while progressing from lower to higher dynamic pressure and Mach number. The subsonic flight region was cleared first before proceeding to the transonic and supersonic flight regions up to a maximum speed of 1.8 Mach. Piloted doublets in the pitch, roll, and yaw axes were performed to excite aircraft responses and obtain postflight parameter estimations of the stability and control derivatives. Maneuvers were typically performed in sets of three, to provide repeatability information.

Although no formal handling qualities evaluations of the spike were conducted during the flight tests, brief pilot commentary was collected for typical piloting and refueling tasks. Aerial refueling with the spike was necessary to prolong flight time during supersonic test conditions. Simple piloting tasks such as climbing, descending, and capturing and maintaining a flight condition were conducted with the CAS both on and off in the subsonic regime (at less than 0.8 Mach) and with the CAS on in the transonic and supersonic regimes.

#### D. Analytical Approach

Before flight-testing of the spike, the baseline F-15B airplane did not have piloted stick and pedal instrumented; consequently, no suitable stability and control data from flight was available for comparison with flight test data obtained with the spike-equipped airplane. Therefore, the effects of the spike installation on the baseline F-15B airplane's stability and control and handling qualities were analyzed entirely with the simulator. Although comparisons were made between the spike-equipped and baseline F-15B airplane over the entire spike flight envelope, three flight conditions, one each in the subsonic, transonic, and supersonic flight region as shown in Table 5, were chosen to show representative results. Identical pitch stick and rudder pedal doublets were chosen for inputs to excite the spike-equipped and baseline airplane simulations. The effects of the spike on F-15B airplane stability and control were analyzed with CAS on and off. Analytical handling qualities comparisons were made with the CAS off in the pitch and yaw axes.

No CAS-on comparison was made because the robust controller corrects for the aerodynamic differences resulting in similar handling qualities. Frequency sweeps were inserted into the simulation and a low-order equivalent system fitting of the resulting frequency response provided estimates of CAP and short period damping for the pitch axis and Dutch roll frequency and damping estimates for the yaw axis.<sup>3</sup>

**Table 5. Representative flight conditions.**

Flight condition	Altitude, ft	Mach number
1	25,000	0.60
2	35,000	0.95
3	45,000	1.80

#### V. Flight Test Results

A total of 30 flights were flown from August 10, 2006, to February 9, 2007, in support of the Quiet Spike flight program. Figure 3 shows the flight conditions flown. The spike flew successfully through the subsonic, transonic, and supersonic flight envelope up to 1.8 Mach in the extended configuration with the CAS on. The F-15B airplane with the attached spike was stable and controllable throughout the flight envelope as predicted by the simulation analyses.<sup>5</sup>

Since the effect of the spike on the roll responses is negligible, the flight test results presented in this report focus on the pitch and yaw axes only. In addition, only the results with the spike in the extended configuration are presented since the retracted configuration results are generally similar or more benign.

##### A. Flight to Simulator Comparisons

The F-15B simulator that was updated with the baseline flight parameter identification results and spike models agreed well with flight data throughout the whole flight envelope. Generally, aircraft response matches were excellent in the pitch and yaw axes for all flight conditions. Typical aircraft response matches are shown in Fig. 4 and Fig. 5 at a transonic condition in the pitch and yaw axes. Comparisons of pitch rate, angle of attack, normal acceleration, symmetric stabilator position, yaw rate, angle of sideslip, and lateral acceleration between flight and simulation match closely. Similar matches were observed in the subsonic and supersonic flight regions. These favorable comparisons validated the stability and control analysis tool and made it easy to safely proceed to the next point.

## B. Stability and Control Derivative Borders

In addition to comparing flight data to simulation, postflight aerodynamic parameter identification data were used to assess the stability and control of the F-15B airplane with the spike. Most of the parameters estimated with PID from flight data were well within the boundary of acceptable aerodynamic variations. Data for the static stability derivative  $C_{m\alpha}$  were generally within the boundaries as shown in Fig. 6. Although  $C_{m\alpha}$  deviated slightly outside the upper boundary at 1.1 Mach, there was little concern since it is still in the stable region. At 1.2 Mach  $C_{m\alpha}$  came back inside the boundaries and remained within the boundaries until 1.8 Mach.

The parameters that showed the most variation from the nominal F-15B values were  $C_{mq}$ ,  $C_{nr}$ , and  $C_{n\beta}$ . The data for  $C_{mq}$  indicated less damping than the nominal F-15B airplane in the subsonic flight region. At the transonic and supersonic conditions, the  $C_{mq}$  projected trend indicated possible deviation outside the acceptable boundary as shown in Fig. 7. The first of these conditions of interest is observed between 1.1 and 1.4 Mach. At that point, data had been collected up to 1.2 Mach at 45,000 ft. The next series of flights expanded the envelope to 1.4 Mach. The trend in the data from 1.2 Mach, extrapolated to 1.4 Mach, indicated that  $C_{mq}$  could fall outside the acceptable region based on the simulation stress analysis. This undesirable projection was identified because it does not follow the nominal F-15B trend, indicated by the dashed line, that shows an increase in damping from 1.1 to 1.2 Mach. Although the projected trend was not considered likely, the simulation was updated for the projected  $C_{mq}$  at 1.4 Mach, and stability margins were recalculated. A piloted simulation evaluation of CAS-off dynamics at this flight condition is shown in Fig. 8. The pilot initiated a 2-g turn, turned the CAS off, and then rolled out to initiate a wings level deceleration to 250 knots, as called for by the CAS-off procedure. The lightly damped response, approximately 0.03 damping, was determined by the pilot to be undesirable, but controllable for this task. As expected, the observed  $C_{mq}$  from flight stayed within the acceptable region and did not follow the projected trend. Flight-estimated  $C_{mq}$  remained at about the 1.2 Mach level of stability, and within the acceptable region, up until just past 1.6 Mach. At that point a destabilizing trend is observed. Projecting this trend to 1.8 Mach and repeating the analysis that was done at 1.4 Mach showed again that stability was acceptable, and that CAS-off dynamics, although undesirable, were controllable. Flight-estimated data at 1.8 Mach verified the projected trend. Fortunately, the goal of the program was achieved at 1.8 Mach, because little margin was left for Mach expansion because of the  $C_{mq}$  results. This method of clearance provided an efficient means for clearing the envelope to the program goal of 1.8 Mach.

Less damping was indicated by  $C_{nr}$  than the nominal F-15B airplane throughout the flight envelope. The variations generally stayed within the previously-defined uncertainty bounds as shown in Fig. 9. Between 1.5–1.6 Mach,  $C_{nr}$  deviated slightly outside the upper boundary. The projected trend for 1.7 and 1.8 Mach conditions indicated  $C_{nr}$  would be slightly outside the upper boundary. The flight test proceeded cautiously at these two flight conditions, however,  $C_{nr}$  flattened out and stayed within the boundaries.

The estimated static stability derivative  $C_{n\beta}$  showed reasonable variations with respect to its boundaries. A rapid reduction in  $C_{n\beta}$  occurred in the 1.2 to 1.3 Mach region as shown in Fig. 10. When extrapolated to 1.4 Mach,  $C_{n\beta}$  deviated to the lower boundary at the next series of expansion points. Flight test continued cautiously, but the flight estimated  $C_{n\beta}$  flattened out at the higher Mach numbers.

### C. Handling Qualities

Pilot commentary indicated that the spike-equipped airplane handled similarly to an F-15B airplane for all tasks in all flight phases. Successful refueling was performed during the course of the program with no handling qualities deficiencies noted.<sup>6</sup> The CAS-off handling qualities in the subsonic regime, less than 0.8 Mach, were adequate for typical piloting tasks. In high-speed flight, at approximately Mach 1.8, the pilot did indicate a bit more "looseness" in the directional axis compared to the F-15B airplane, but he did not feel it was a significant handling qualities deficiency. Although comparisons of rudder doublets of the simulation with and without the spike in Fig. 11(b) show very little deviation with the CAS on, CAS-off comparisons in Fig. 12 show small, relatively mild reductions in Dutch roll damping caused by the spike. Figure 13 shows Dutch roll frequency and damping estimates for the three flight conditions in Table 3. These results were generated with a linear model updated with parameter-estimated data for the spike extended. The small reductions in Dutch roll damping because of the spike are not significant enough to cross into the level 2 region.

### D. Analytical Results

Pitch-axis handling qualities analysis of the baseline F-15B airplane and the F-15B spike configuration with the CAS off are summarized in Fig. 14. Generally, short period damping has been modified, while the CAP remains relatively unaffected. For the test point at 25,000 ft and 0.6 Mach, the reduction is within the level 2 region and not significant. This corresponds to the adequate CAS-off handling qualities indicated in flight experience. Short period damping increases in the transonic region. This is consistent with parameter estimation where  $C_{m_q}$  becomes more negative than the baseline airplane at 0.95 Mach (see Fig. 7). At 1.8 Mach, however, where the damping is quite low for the baseline airplane, the spike contributes an approximate 33 percent reduction in short period damping. This level of reduction in damping was determined in piloted simulation to be marginally acceptable for a level deceleration task that was added as an addendum to emergency procedures for a CAS-off event.

The effect of the spike on the stability and control of the F-15B airplane was minimal. With the CAS on, the pitch and yaw responses with and without the spike extended were nearly identical as shown in Fig. 11 for the 1.8 Mach flight condition. The similar responses were attributed to the robustness of the CAS, the relatively small aerodynamic effect of the spike on the overall aerodynamic characteristics of the F-15B airplane, and negligible changes in the location of the center of gravity and moment of inertia characteristics. With the CAS off, there were more noticeable effects of the spike in the pitch and yaw axes. In the yaw axis, the damping ratios were reduced for all three conditions in Table 3 with the spike. At 0.95 Mach, larger magnitude oscillations were observed as shown in Fig. 15(a). In the pitch axis, there were minimal effects in the subsonic and transonic regime. In the supersonic flight region, however, the pitch damping is much less, as shown in Fig. 15(b).

## VI. Conclusions

Flight-testing of the F-15B Quiet Spike program was successfully completed in February 2007. The spike flight envelope was cleared without incident in the fully extended and retracted configurations. Extensive preflight simulation analyses indicated adequate stability margins and handling qualities. The stability and control flight envelope clearance was accomplished by evaluating flight data against the simulator analysis results. Excellent matches in aircraft dynamic responses were observed between flight and simulation. Generally, postflight parameter estimations of the aerodynamic derivatives were within the uncertainty-bounded regions of acceptable aerodynamic variations. A few trends indicated possible deviations outside the acceptable aerodynamic variations that required piloted simulation evaluation to show adequate stability, controllability and handling qualities before conducting flight tests at the next conditions. The effect of the spike on the stability and control with the CAS on was negligible. With the CAS off, the CAP remains relatively unaffected from the nominal F-15B airplane, whereas short period damping was slightly modified. The short period damping was unaffected in the subsonic region, increased in the transonic region, and decreased in the supersonic region. Although the short period damping was slightly affected, it still remains within the same CAP level. Pilot commentary indicated that the augmented airplane handled similarly to an F-15B airplane for all required tasks in all flight phases. Successful refueling was performed with the spike extended during the course of the program with no deficiencies noted.

## VII. References

- <sup>1</sup> Richwine, D. M., "F-15B/Flight Test Fixture II: A Test Bed for Flight Research," NASA TM 4782, 1996.
- <sup>2</sup> Cumming, S. B., Smith, M. S., and Frederick, M., "Aerodynamic Effects of an Oversized, Multi-Segmented Nose Boom on an F-15B," AIAA-2007-6638, *AIAA Atmospheric Flight Mechanics Conference*, Hilton Head, South Carolina, August 20, 2007.
- <sup>3</sup> McWherter, S., Moua, C., Cox, T., and Gera, J., "Stability and Control Analysis of the F-15B Quiet Spike Aircraft," NASA TM, 2007 (to be published).
- <sup>4</sup> *Flying Qualities of Piloted Vehicles*, U.S. Department of Defense, MIL-STD 1797, March 31, 1987.
- <sup>5</sup> Moua, C., McWherter, S., Cox, T., and Gera, J., "Flight Test Results on the Stability and Control of the F-15B Quiet Spike Aircraft," NASA TM, 2007 (to be published).
- <sup>6</sup> Smolka, J. W., Cowart, R. A., Molzahn, L. M., et al, "Flight Testing of the Gulfstream Quiet Spike™ on a NASA F-15B," *Society of Experimental Test Pilots 51<sup>st</sup> Symposium and Banquet*, Anaheim, California, September 26–29, 2007.

## Figures



Figure 1. The F-15B test bed airplane with extended Quiet Spike.

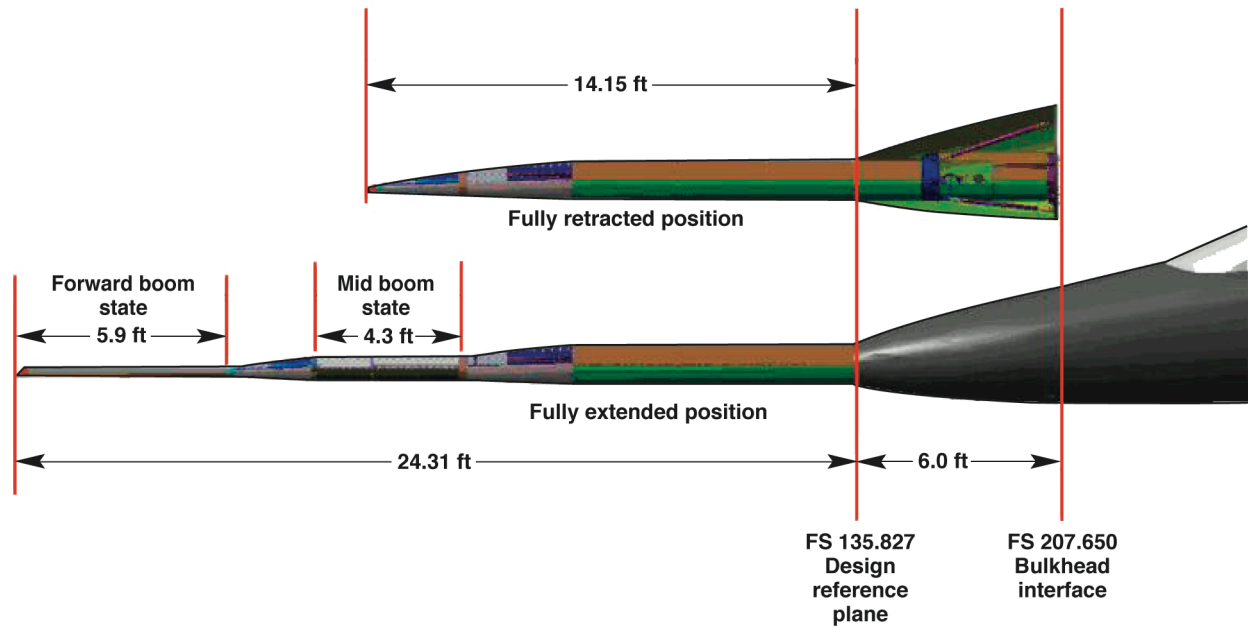


Figure 2. The Quiet Spike boom configuration.

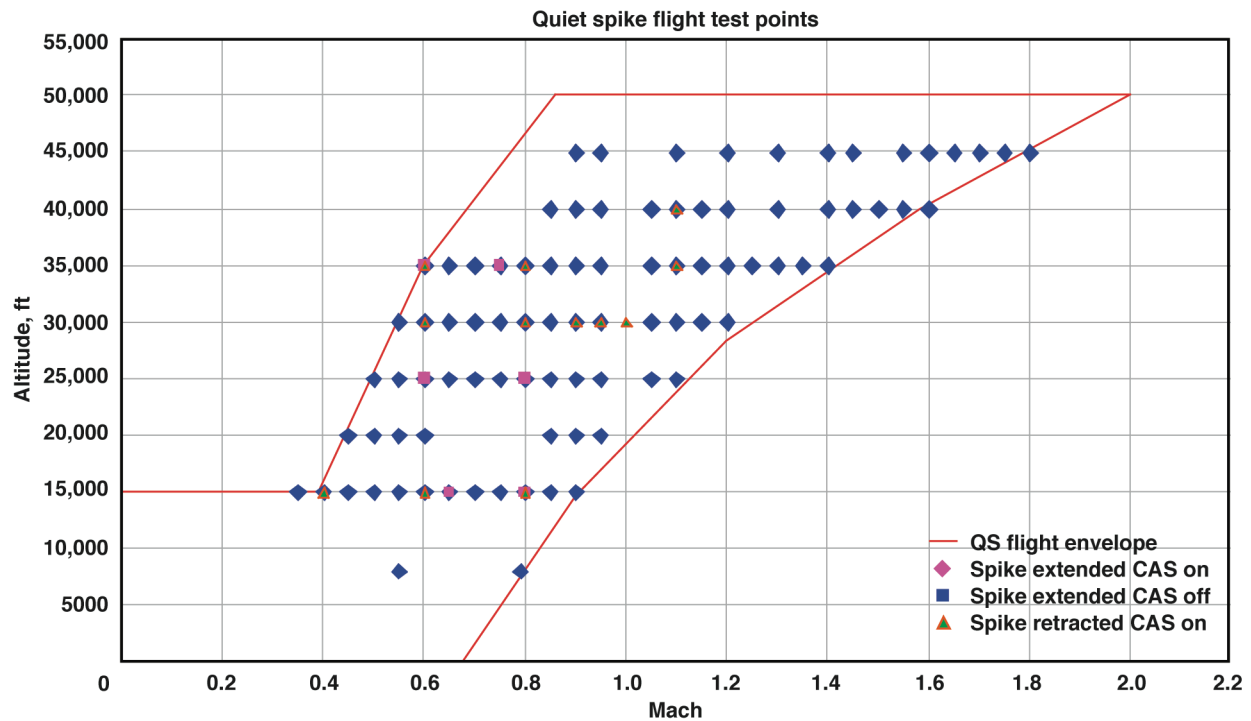
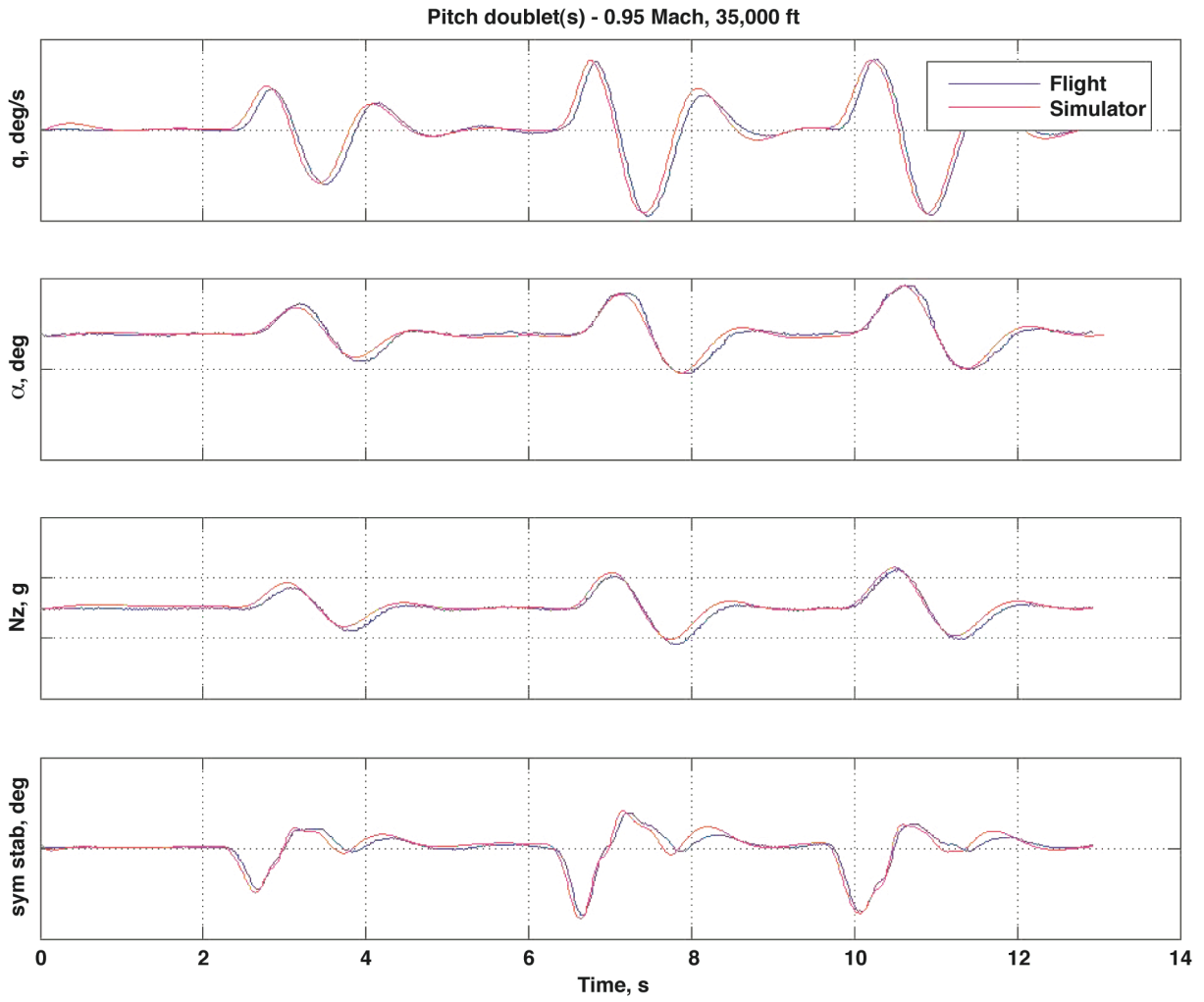


Figure 3. Quiet Spike flight test points.



**Figure 4. Pitch doublets in the transonic region.**

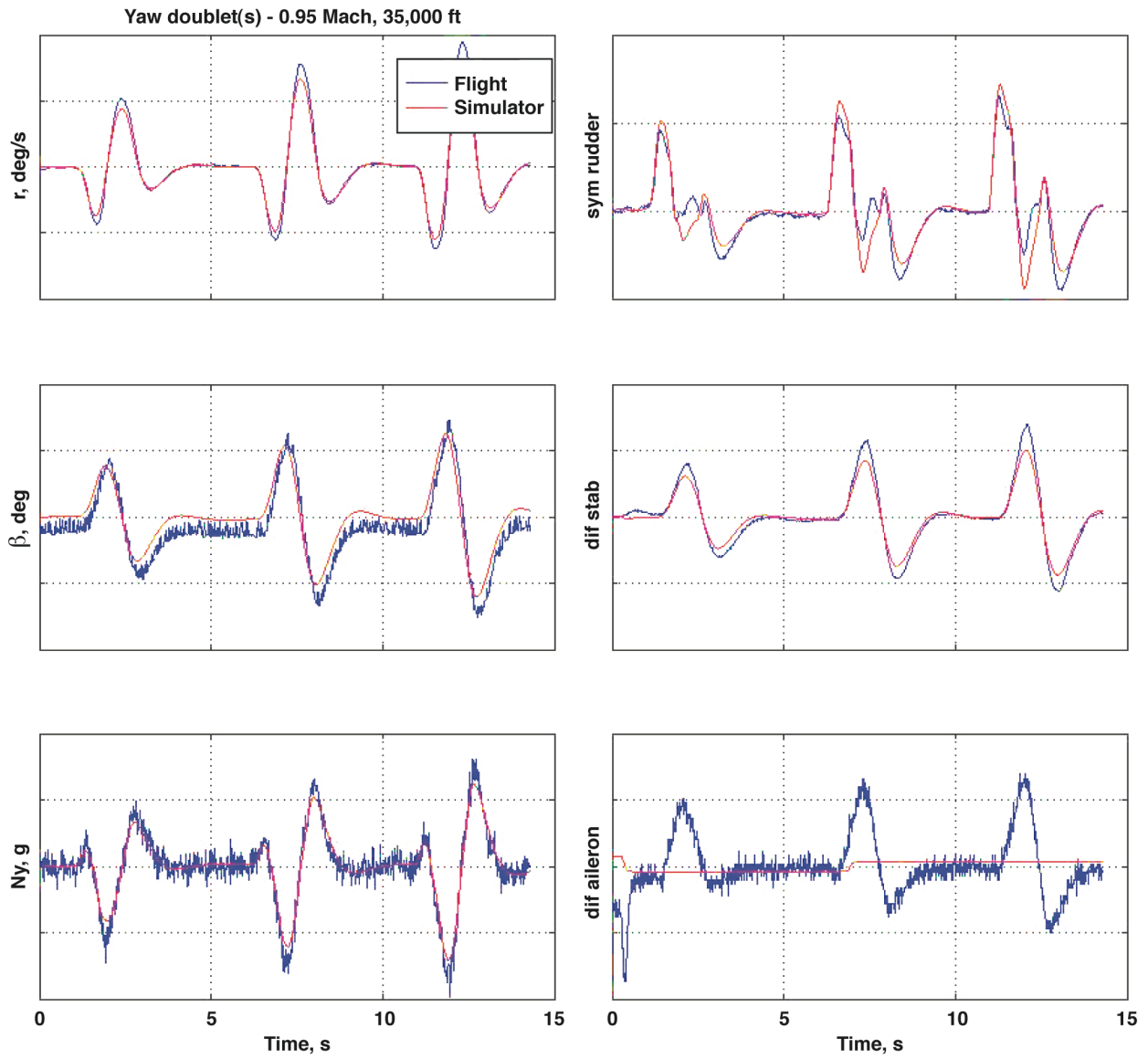


Figure 5. Yaw doublets in the transonic region.

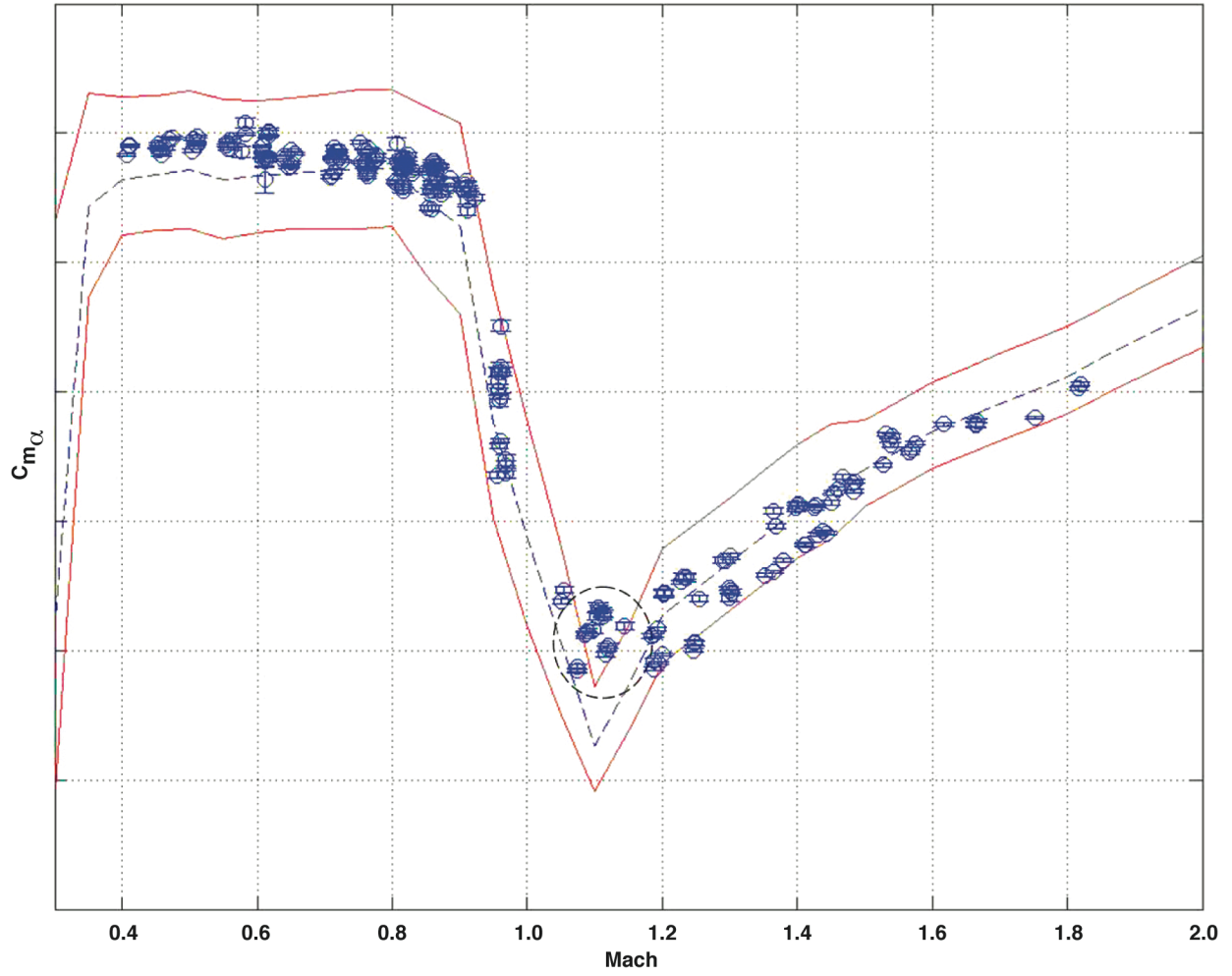


Figure 6. Stability and control derivative -  $C_{m\alpha}$ .

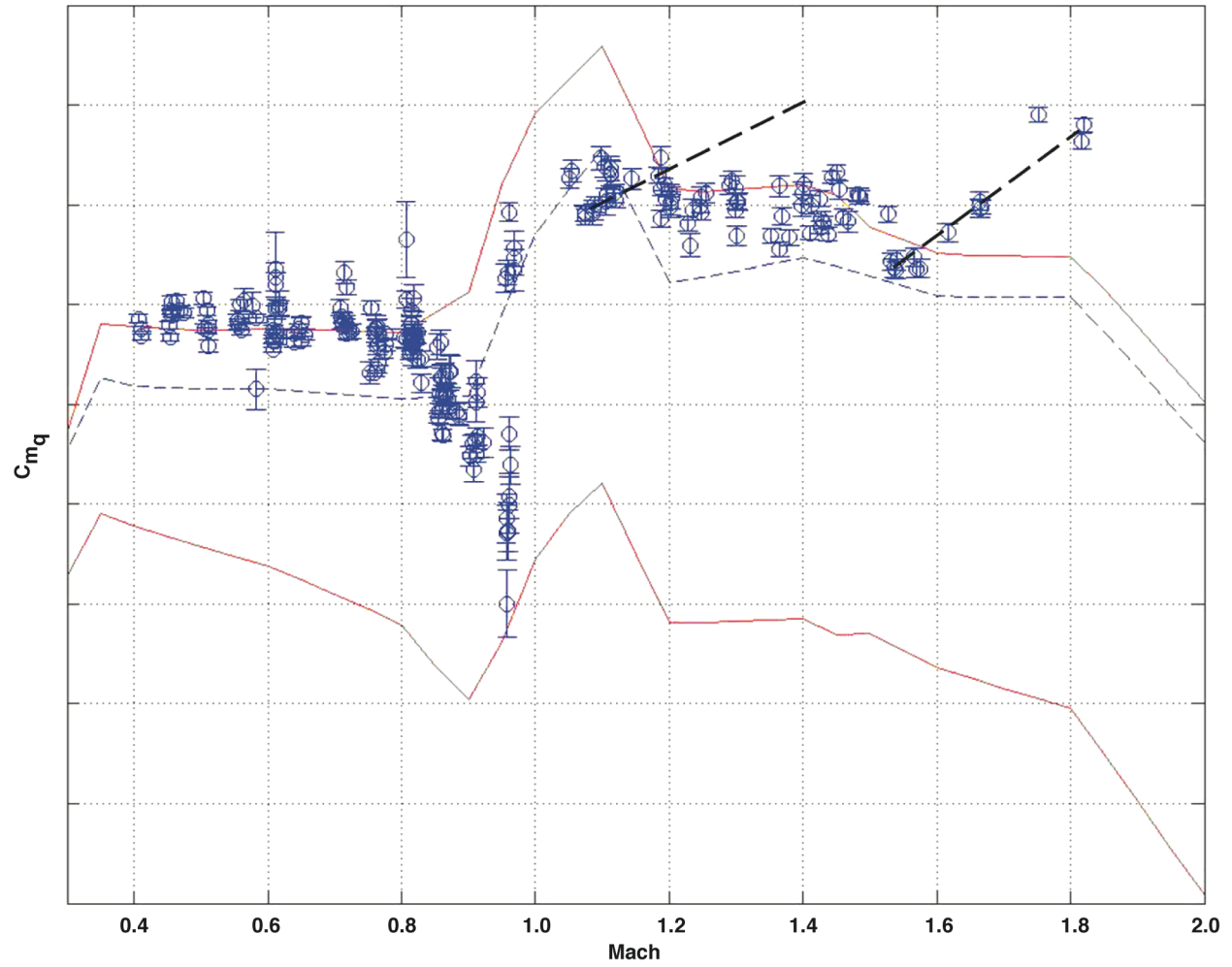


Figure 7. Stability and control derivative -  $C_{m_q}$ .

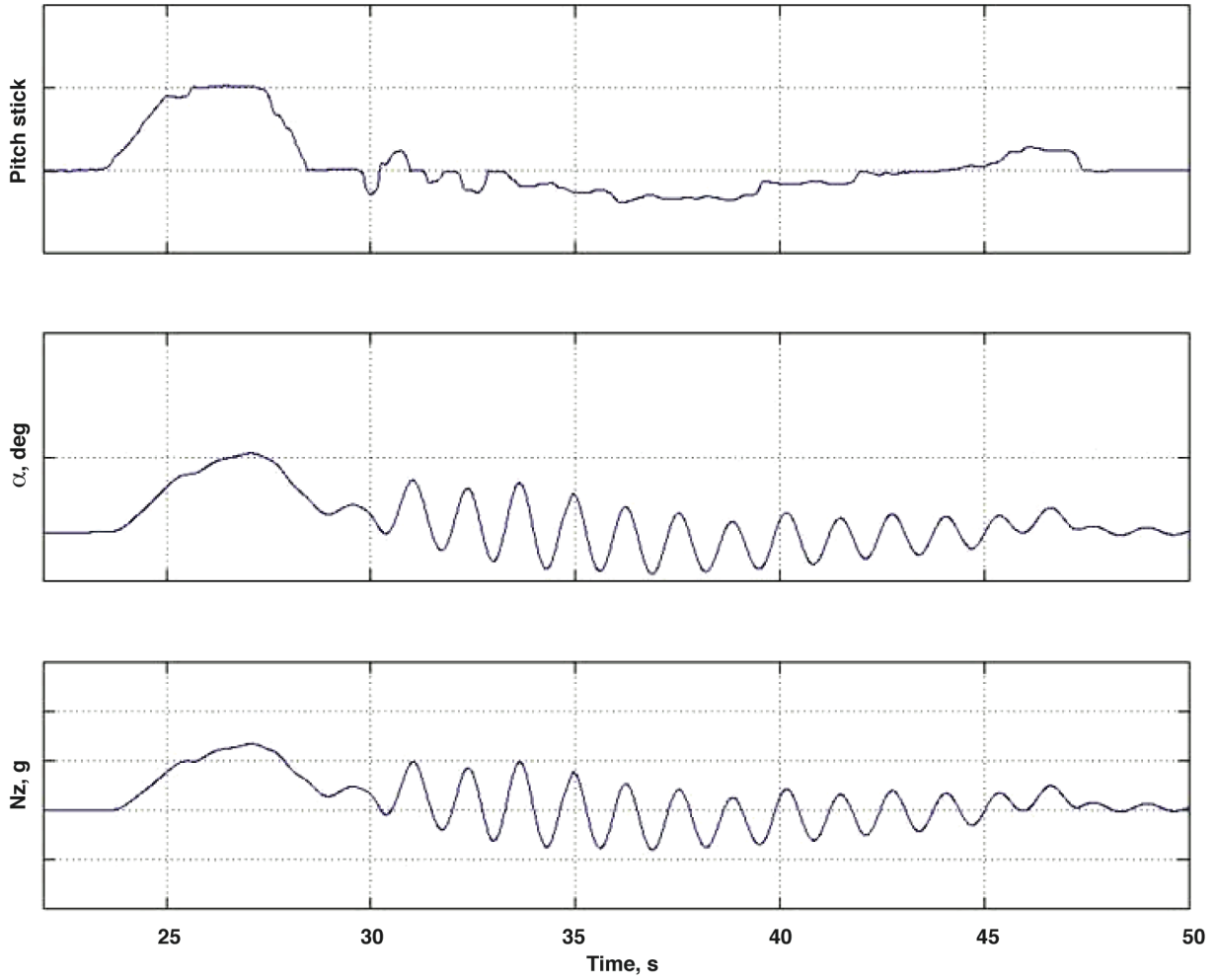


Figure 8. Piloted evaluation at 1.4 Mach.

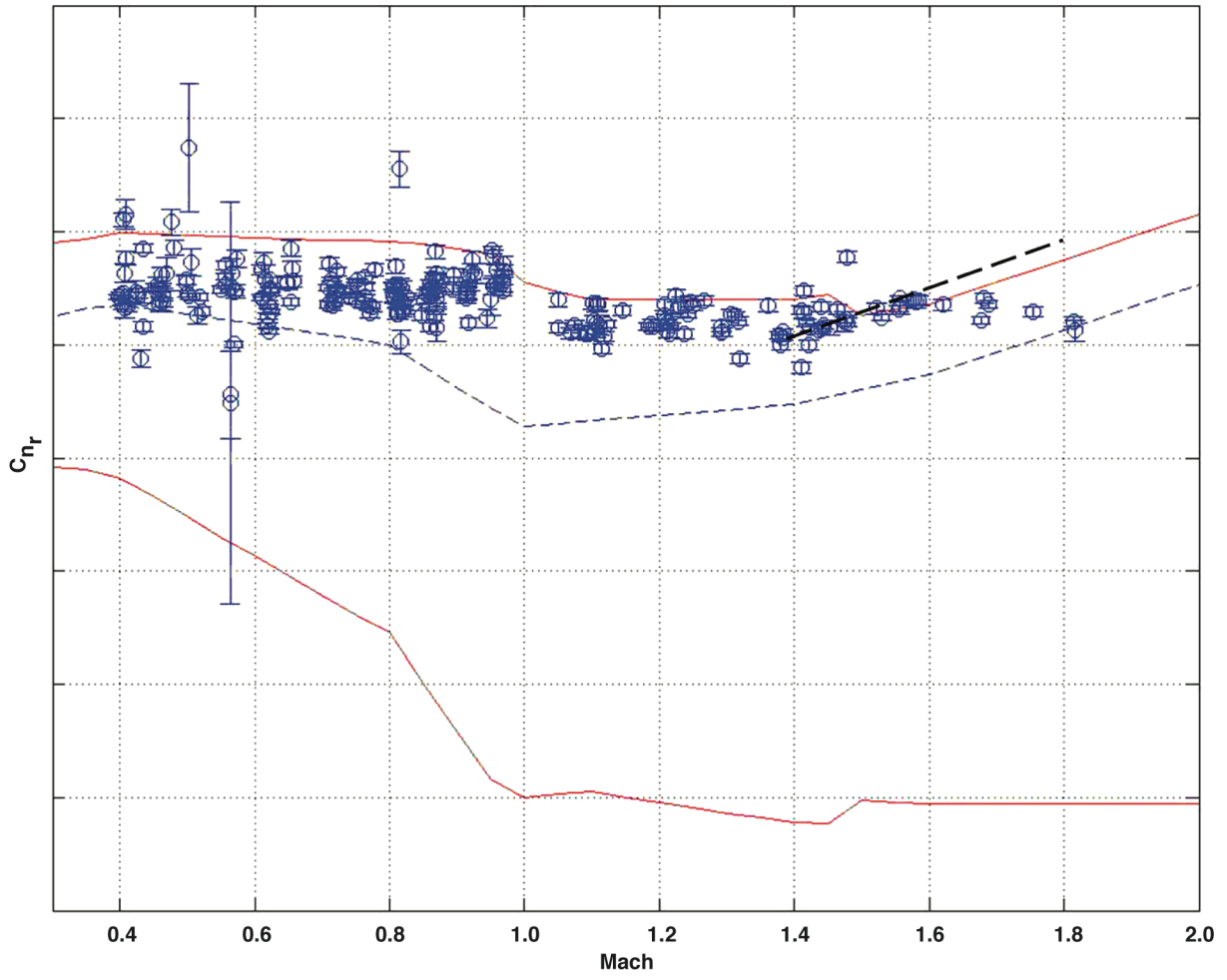


Figure 9. Stability and control derivative -  $C_{nr}$  .

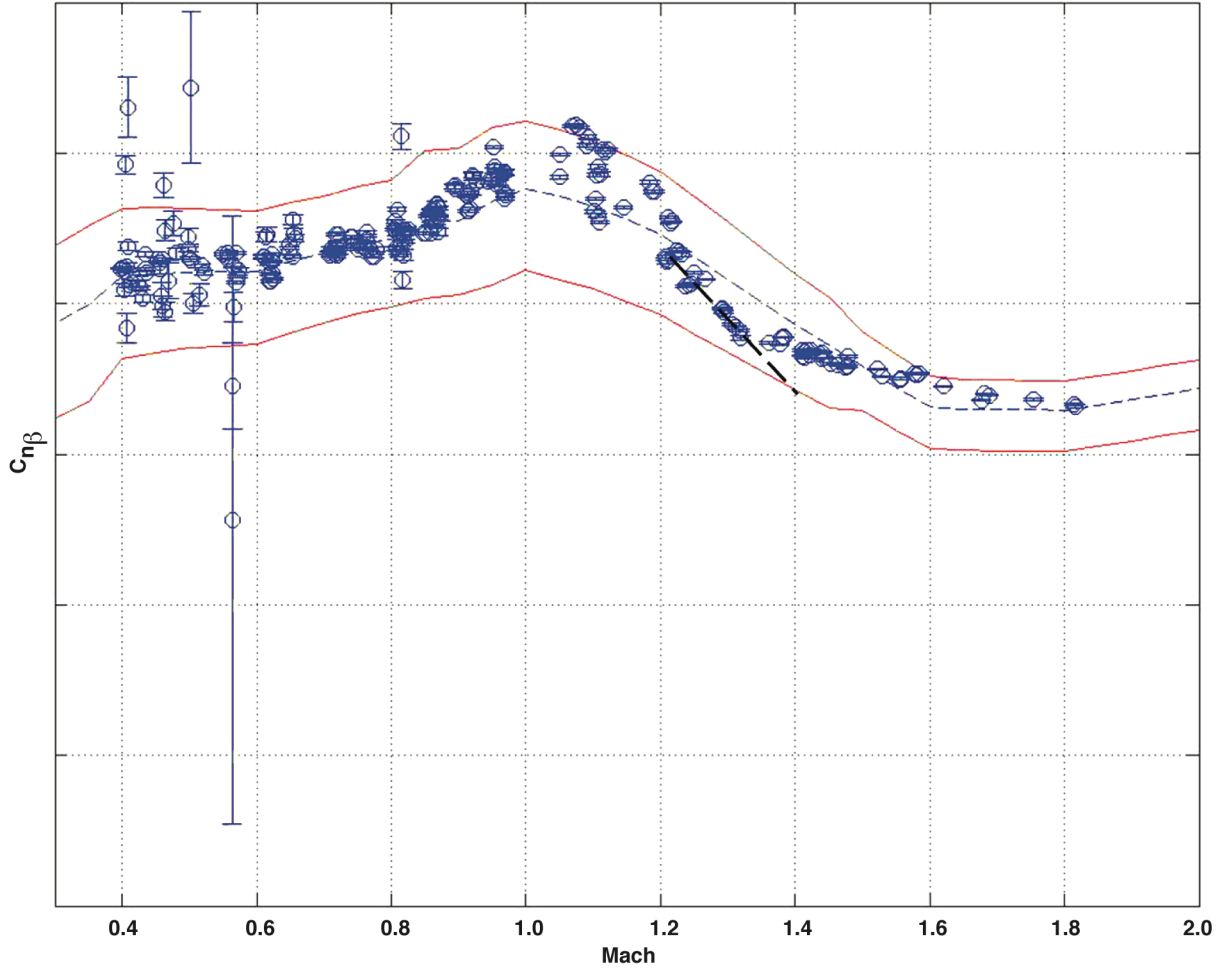


Figure 10. Stability and control derivative -  $C_{n\beta}$ .

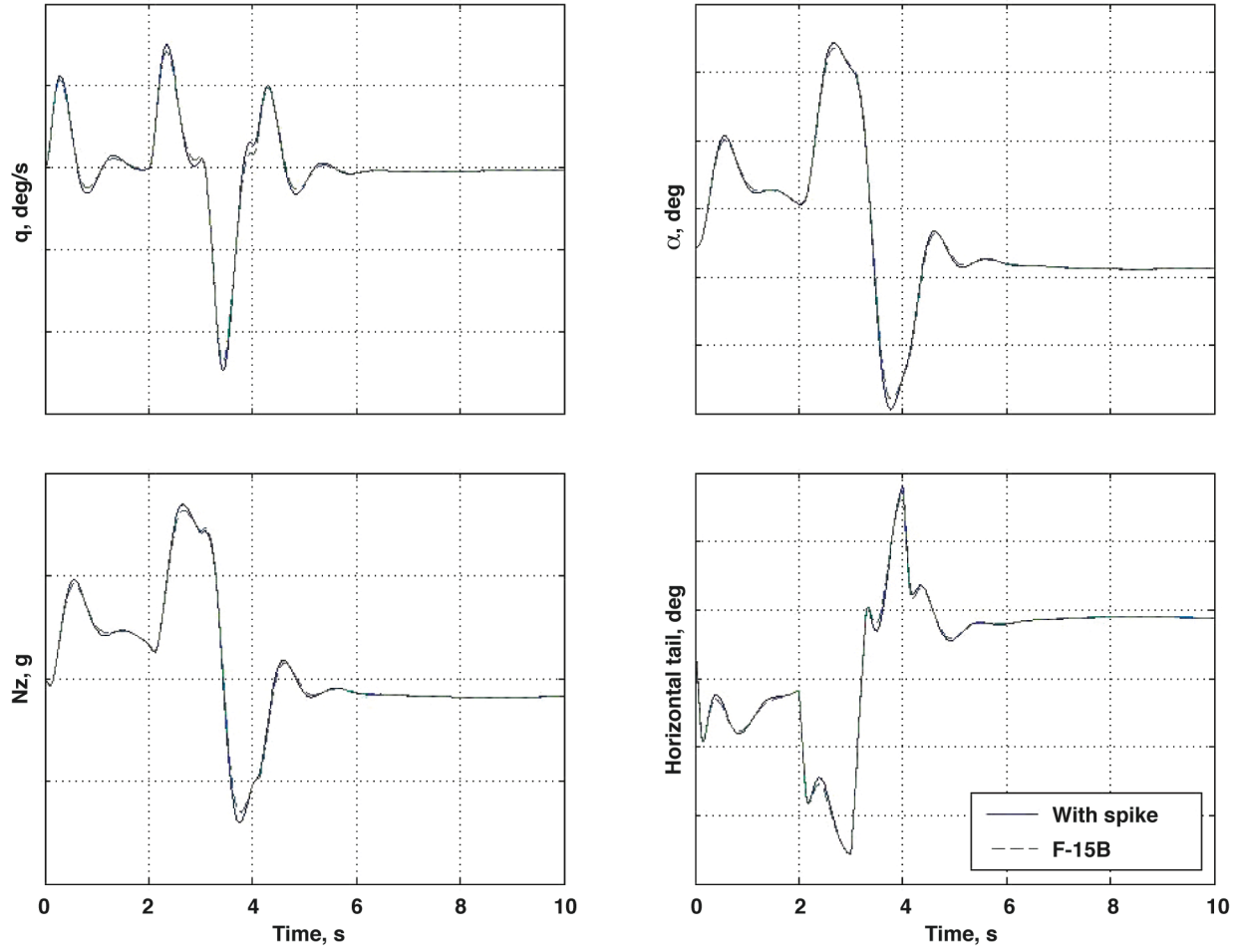


Figure 11(a). Pitch stick doublet.

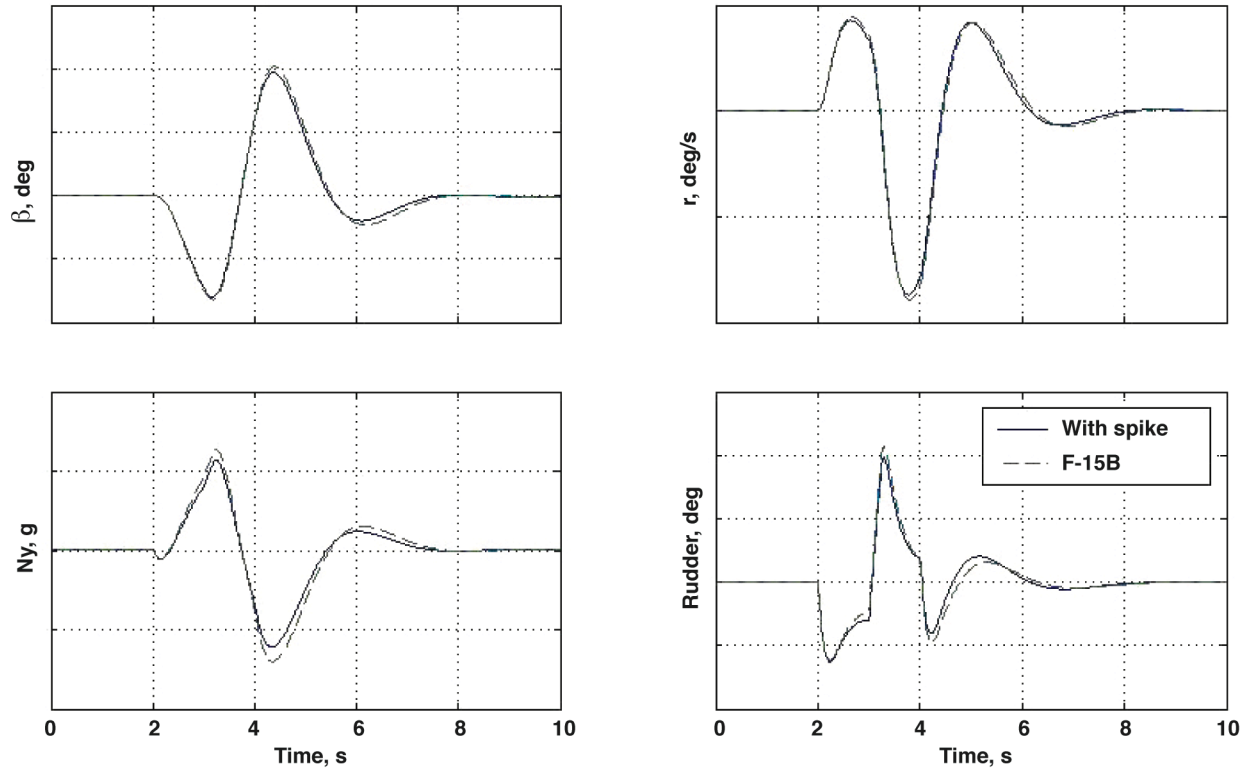


Figure 11(b). Rudder pedal doublet.

Figure 11. The CAS-on comparison of the responses of the test configuration with the baseline F-15B airplane at flight condition 3.

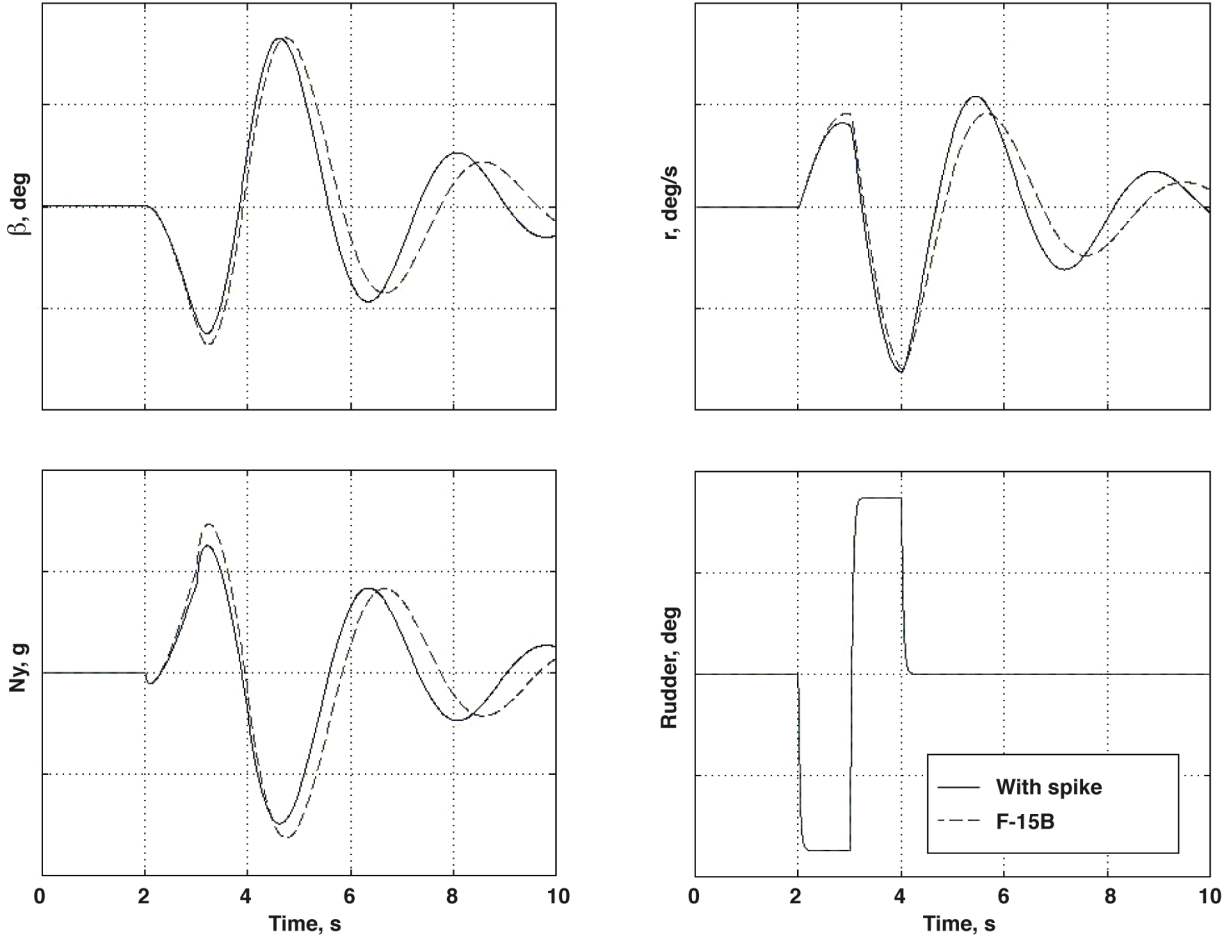


Figure 12. The CAS-off comparison of the responses of the test configuration with the baseline F-15B airplane at flight condition 3 using rudder pedal doublet.

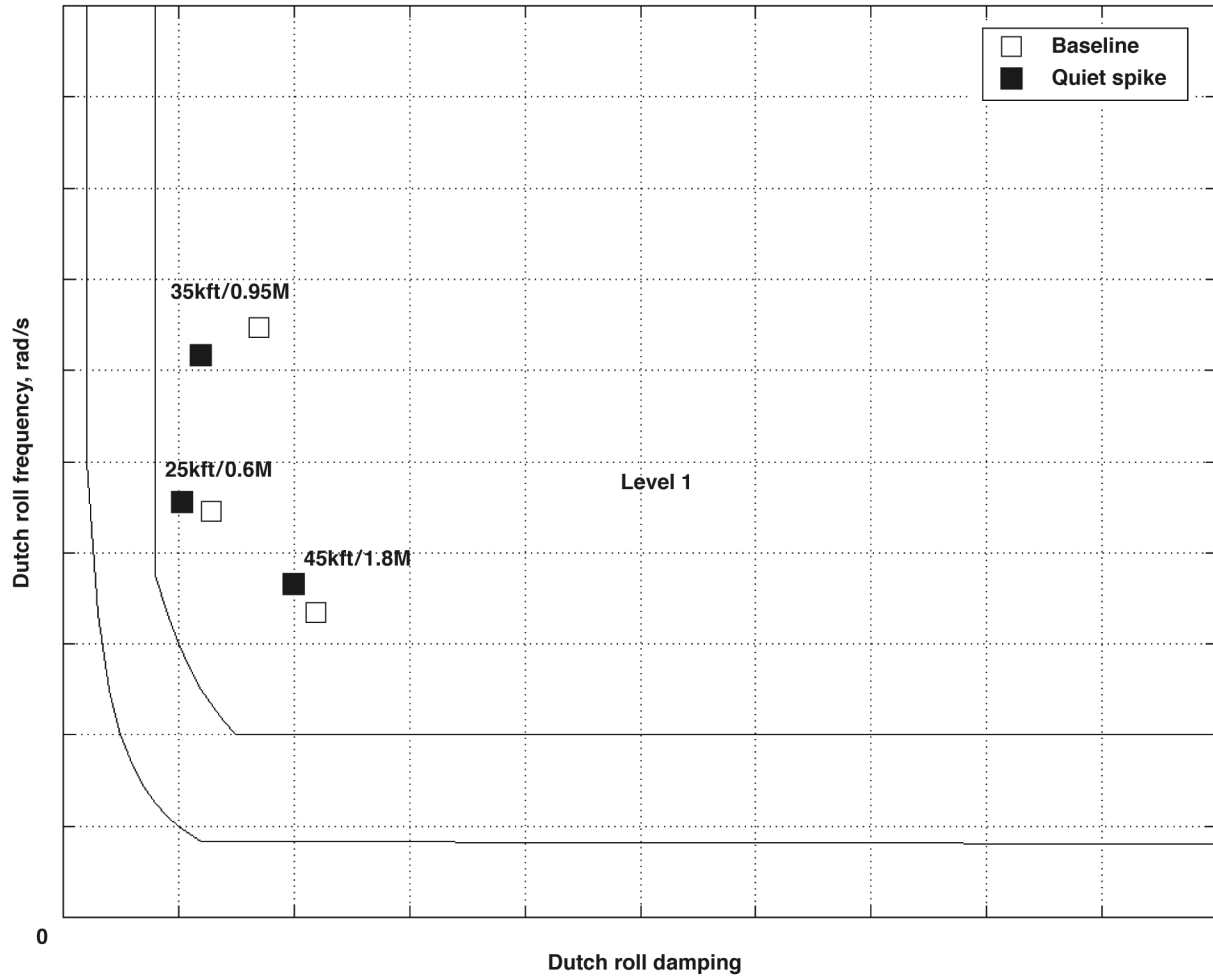
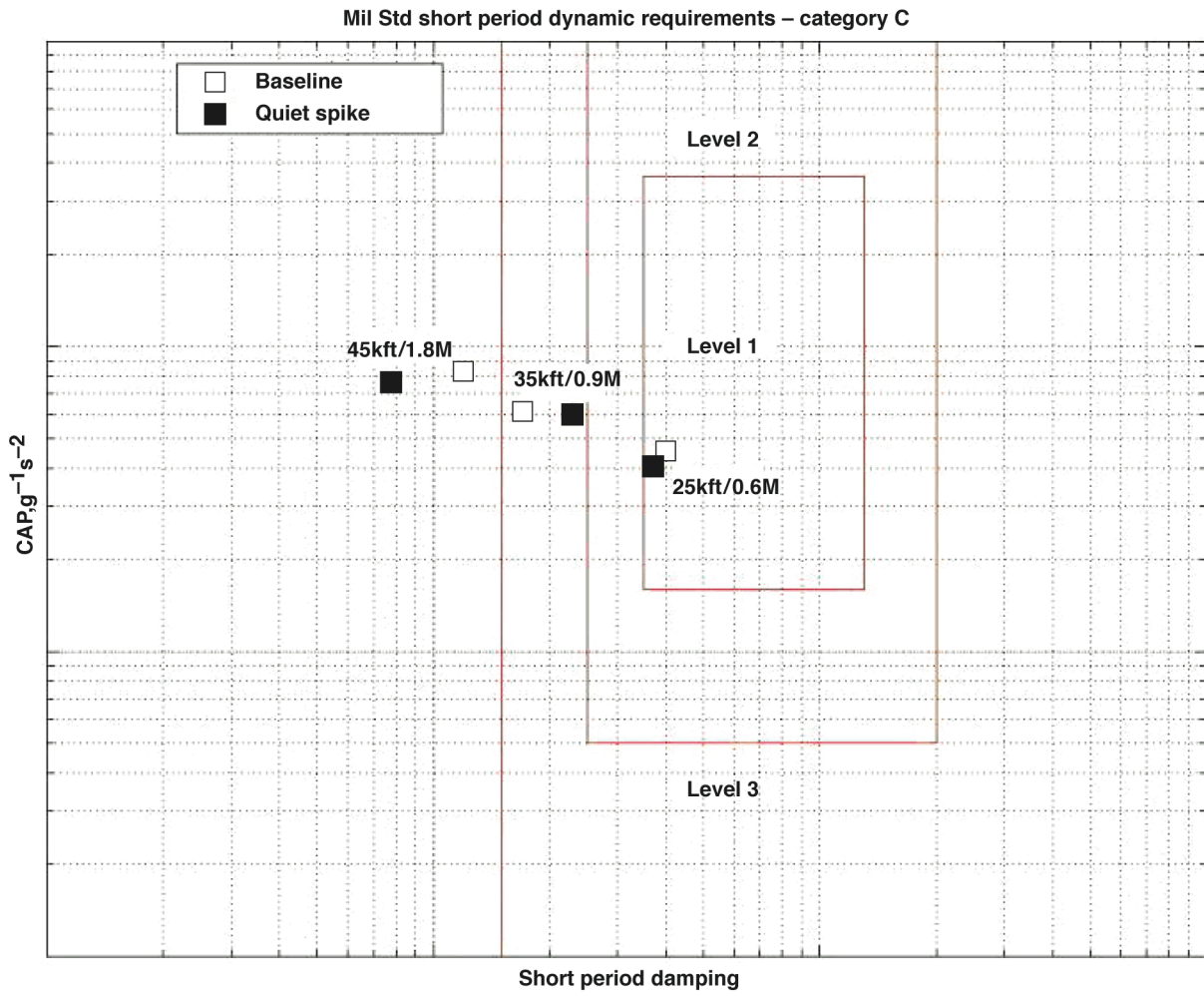


Figure 13. The CAS-off yaw axis handling qualities evaluation of flight conditions 1, 2, and 3.



**Figure 14. The CAS-off pitch axis handling qualities evaluation of a subsonic, transonic, and supersonic flight condition.**

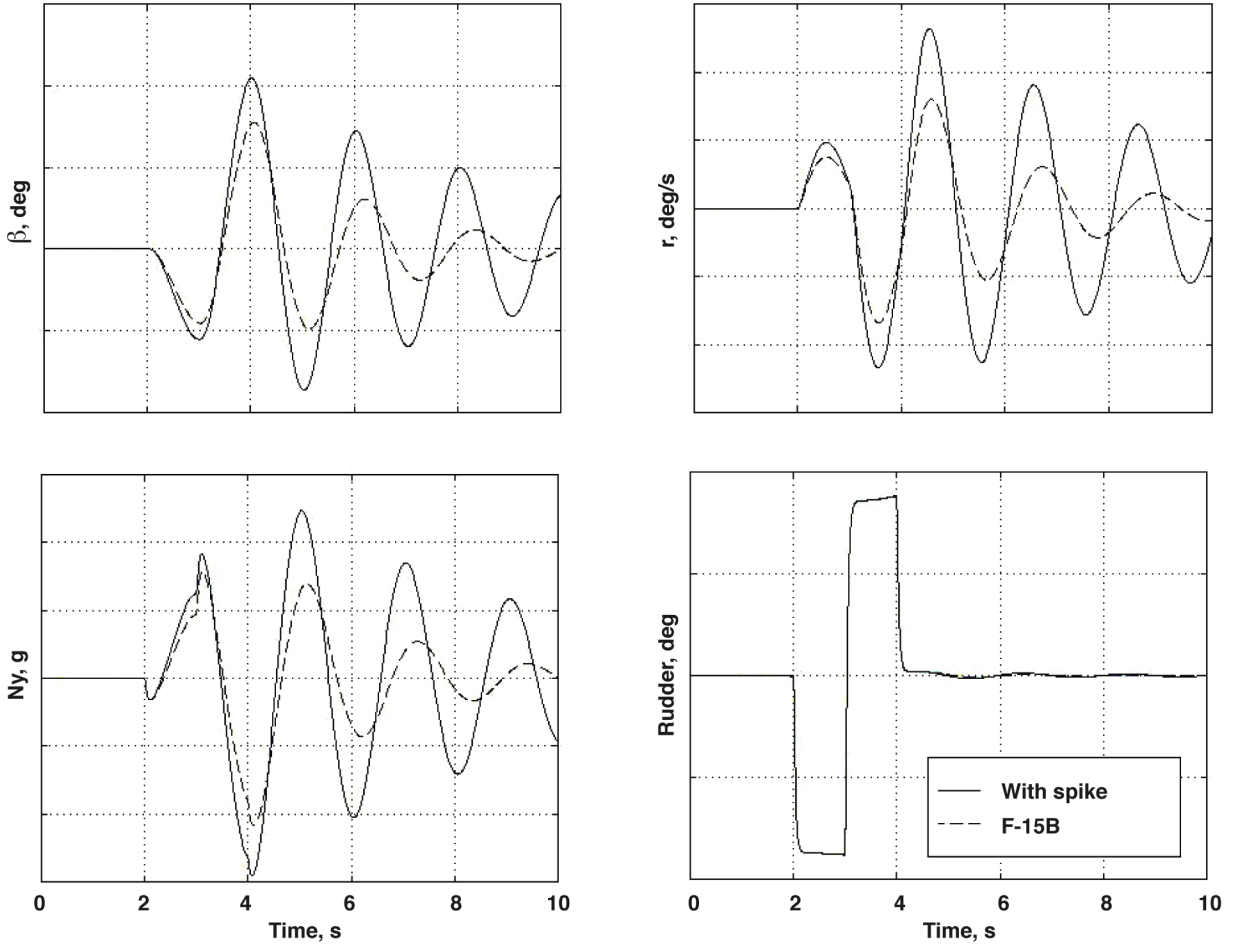


Figure 15(a). Rudder pedal doublet.

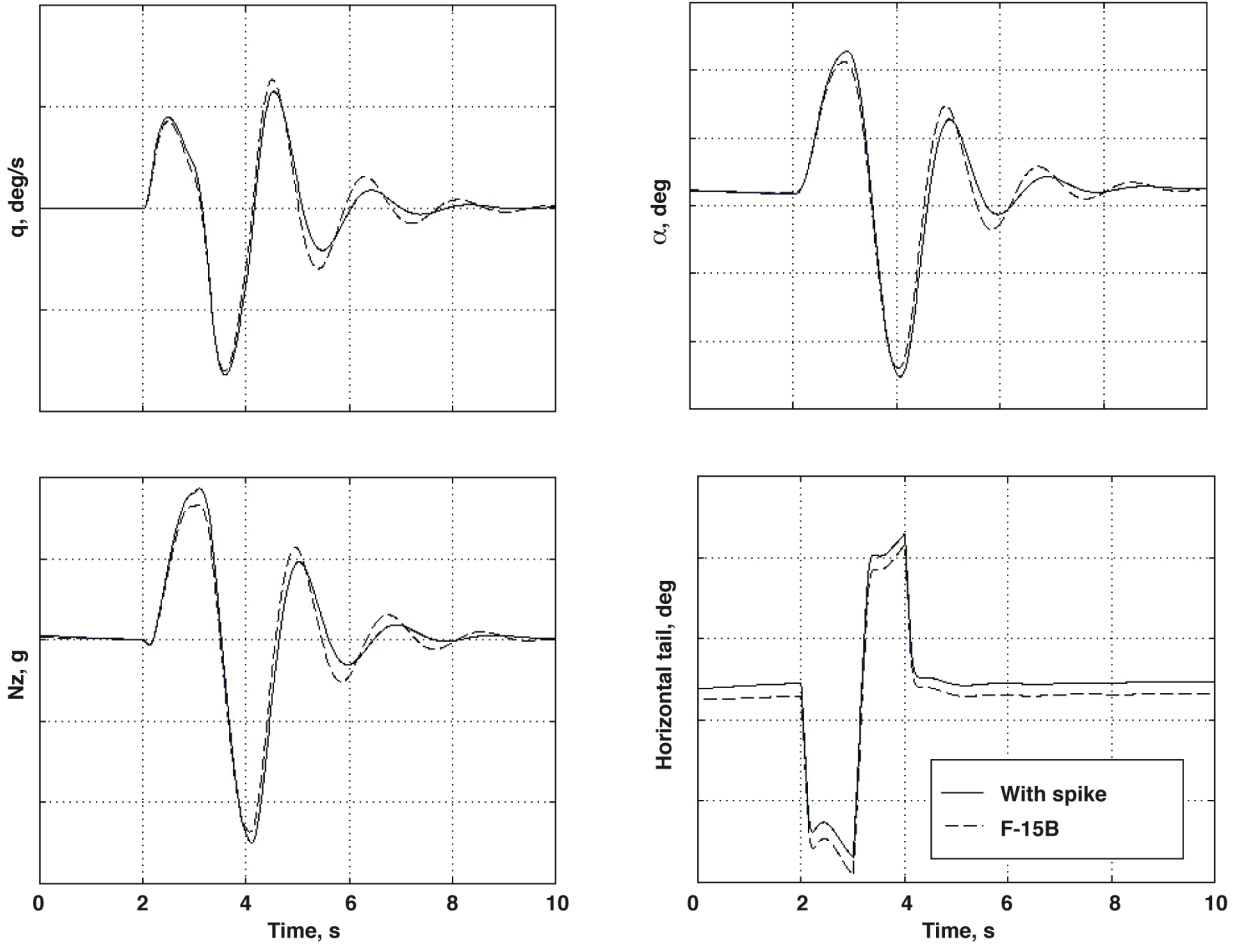


Figure 15(b). Pitch stick doublet.

Figure 15. The CAS-off comparison of the responses of the test configuration with the baseline F-15B airplane at flight condition 2.